Gene Therapy (2018) **25**, 54–65

www.nature.com/gt

OPEN

ORIGINAL ARTICLE

Efficacy of combining ING4 and TRAIL genes in cancer-targeting gene virotherapy strategy: first evidence in preclinical hepatocellular carcinoma

A Galal El-Shemi[1,2], A Mohammed Ashshi[1], E Oh[3], B-K Jung[3], M Basalamah[1,4], A Alsaegh[1] and C-O Yun[3]

Current treatments of hepatocellular carcinoma (HCC) are ineffective and unsatisfactory in many aspects. Cancer-targeting gene virotherapy using oncolytic adenoviruses (OAds) armed with anticancer genes has shown efficacy and safety in clinical trials. Nowadays, both inhibitor of growth 4 (ING4), as a multimodal tumor suppressor gene, and tumor necrosis factor-related apoptosis-inducing ligand (TRAIL), as a potent apoptosis-inducing gene, are experiencing a renaissance in cancer gene therapy. Herein we investigated the antitumor activity and safety of mono- and combined therapy with OAds armed with ING4 (Ad-ΔB/ING4) and TRAIL (Ad-ΔB/TRAIL) gene, respectively, on preclinical models of human HCC. OAd-mediated expression of ING4 or TRAIL transgene was confirmed. Ad-ΔB/TRAIL and/or Ad-ΔB/ING4 exhibited potent killing effect on human HCC cells (HuH7 and Hep3B) but not on normal liver cells. Most importantly, systemic therapy with Ad-ΔB/ING4 plus Ad-ΔB/TRAIL elicited more eradicative effect on an orthotopic mouse model of human HCC than their monotherapy, without causing obvious overlapping toxicity. Mechanistically, Ad-ΔB/ING4 and Ad-ΔB/TRAIL were remarkably cooperated to induce antitumor apoptosis and immune response, and to repress tumor angiogenesis. This is the first study showing that concomitant therapy with Ad-ΔB/ING4 and Ad-ΔB/TRAIL may provide a potential strategy for HCC therapy and merits further investigations to realize its possible clinical translation.

Gene Therapy (2018) **25,** 54–65; doi:10.1038/gt.2017.86

INTRODUCTION

Hepatocellular carcinoma (HCC) is a multi-factorial liver cancer presently accounting for the second leading cause of cancer-related deaths worldwide.[1,2] At the therapeutic level, HCC is classified as a highly chemo- and radio-resistant cancer.[1,2] In addition to that, the therapeutic-, survival- and safety benefits of its recently FDA-approved molecular target drugs (for example, sorafenib) are still far from being satisfied.[2] Also, liver transplantation, surgical and other non-surgical treatment options that may provide curative option are only feasible in patients with initial stages, and due to a late diagnosis, most of HCC patients cannot be subjected to such therapy.[1,2] Thus, there is an imperative demand to explore new alternative therapies. Combinatorial therapeutic approaches with multi-tumoricidal mechanisms may have significant advantages for treatment of human HCC. At this end, utilization of cancer-targeting gene virotherapy mediated by oncolytic adenoviruses (OAds) armed with anticancer transgenes is being the most potential strategy in this setting.[3–5] In this sense, hundreds of HCC patients have been in clinical trials based on this novel therapeutic approach with encouraging data in terms of tolerability, safety profile and early signs of efficacy.[4,5]

Gene therapy emerged as a distinguished tool to cure human diseases including cancers that would be untreatable by conventional drugs. In gene-based cancer therapy, replication-deficient adenoviruses have been widely used to deliver anticancer genes of interest; however, their non-replicative property, unsuccessful amplification in tumor cells and transfect both tumor and normal cells have hindered their positive clinical translation. As a logical consequence, conditionally replicating OAds, which preferentiality and selectively replicate in- and lyse cancer cells while sparing normal cells, have been generated and their safety record has been clinically approved.[3–5] Nonetheless, therapeutic trials based on OAd alone was shown to be less effective to eradicate tumors with sophisticated hostile barriers and complexed tumor microenvironment. To overcome such limitations and strength their anticancer efficacy, OAds were subsequently modified to be armed with a potential tumor suppressor-, pro-apoptotic-, immunomodulatory-, antiangiogenic- or another anticancer/suicide gene, providing a new era of cancer-targeting gene virotherapy.[5–7] More specifically, further enforcement of this strategy to simultaneously deliver dual antitumor genes acting together with distinct mechanisms has suggested to provide a more meaningful therapeutic maneuver via triplex interactions between the viral lytic effect and the additive/augmenting antitumor effects of the co-expressed genes.[7–11]

Triggering of apoptosis in tumor cells seemed to be a hopeful weapon in apoptosis-mediated cancer therapy.[1] With this aim, tumor necrosis factor-related apoptosis inducing ligand (TRAIL) has drawn considerable attention as a potent and safe apoptotic ligand able to induce fulminant apoptosis in HCC and several human cancer cells with almost nontoxic effects on normal cells.[12–14] TRAIL-based gene therapy was also shown to produce profound apoptosis in tumor cells but not in normal cells,[13–15] and tumor-specific TRAIL expression mediated by OAd may provide a

[1]Department of Laboratory Medicine, Faculty of Applied Medical Sciences, Umm Al-Qura University, Holy Makkah, Saudi Arabia; [2]Department of Pharmacology, Faculty of Medicine, Assiut University, Assiut, Egypt; [3]Department of Bioengineering, College of Engineering, Hanyang University, Seoul, Korea and [4]Department of Pathology, Faculty of Medicine, Umm Al-Qura University, Holy Makkah, Saudi Arabia. Correspondence: Professor C-O Yun, Department of Bioengineering, College of Engineering, Hanyang University, 222 Wangsinmi-ro, Seongdong-gu, Seoul 04763, Korea.
E-mail: chaeok@hanyang.ac.kr

Received 26 February 2017; revised 31 August 2017; accepted 11 September 2017; accepted article preview online 19 September 2017; advance online publication, 18 January 2018

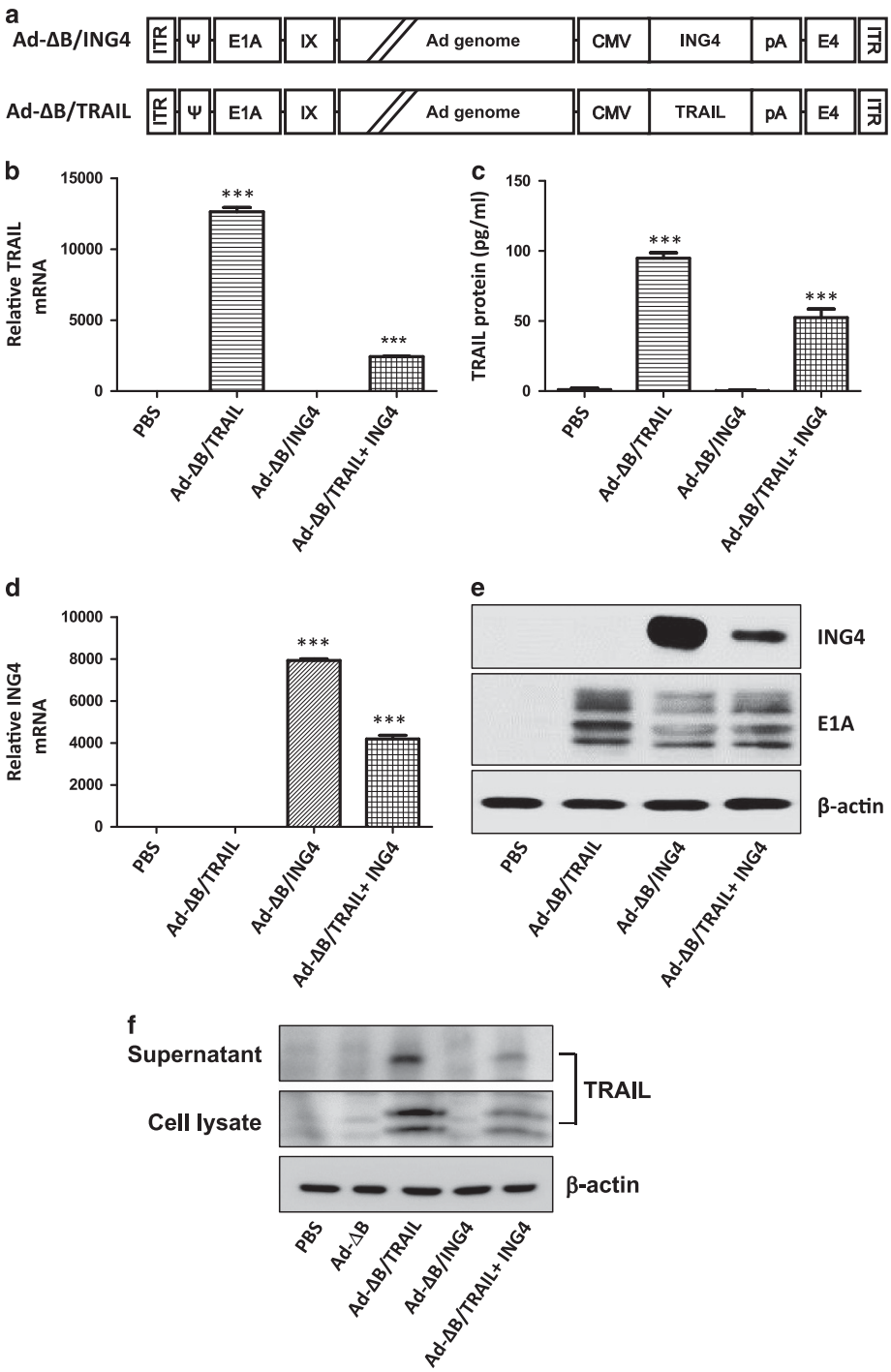

Figure 1. Validation of *TRAIL* and *ING4* gene expression in human HCC cells treated with Ad-ΔB/TRAIL and/or Ad-ΔB/ING4. (**a**) Schematic representation of genomic structure of generated oncolytic adenovirus (Ad-ΔB) armed with human *ING4* gene (Ad-ΔB/ING4) or human *TRAIL* gene (Ad-ΔB/TRAIL). *ING4* or *TRAIL* gene was incorporated in the E3 region of the viral backbone under the transcriptional control of the human cytomegalovirus (CMV) promoter. Next, viral replication and gene expression pattern of TRAIL and ING4 was validated on human HCC HuH7 cells treated with PBS, Ad-ΔB/TRAIL, Ad-ΔB/ING4 or Ad-ΔB/TRAIL + ING4 at a MOI of 5 for each virus. The harvested cells and their supplements were analyzed by qRT-PCR to measure the relative mRNA of TRAIL (**b**) and ING4 (**d**), ELISA; to measure TRAIL protein (**c**) and western blot (**e** and **f**); to measure the expression level of ING4, TRAIL and Ad production by measuring E1A protein. Data of (**b**–**d**) are represented as mean ± s.e. ***$P < 0.001$ versus PBS.

novel therapeutic approach for treatment of advanced and complexed cancers.[15] In despite of this, the importance of combining *TRAIL* gene-based therapy with other potential anticancer genes/agents was strongly supposed to improve the overall antitumor efficacy and to overcome the development of cancer cell resistance toward TRAIL.[8,10,14]

In a constant line, inhibitor of growth 4 (ING4) is an emerged multimodal tumor suppressor gene of ING family that its expression is downregulated or even completely lost in various human cancers including HCC.[16,17] Moreover, low expression of ING4 in liver tumor tissues of patients with HCC is significantly correlated with rapid cancer progression and patient poor

prognosis.[18] Based on these facts, ING4 has been raised as a potential candidate in the era of gene-based cancer therapy.[19] At that respect, delivery of *ING4* gene via adenoviral vectors into HCC,[20,21] lung carcinoma,[22] colorectal cancer,[23] osteosarcoma,[24] hypopharngeal cancer[25] and other modalities human cancers, was found to not only inhibit tumor growth, angiogenesis and invasion, but also regulate cell proliferation and apoptosis and facilitate tumor cell sensitivity to other adjuvant anticancer agents.[19–25] Nevertheless, most of these previous trials were based on using the traditional replication-deficient adenoviral vector to deliver *ING4* gene, and their data were collectively highlighted the importance of combining *ING4* gene with additional antitumor gene or chemotherapeutic drugs to achieve more potent antitumor effects than *ING4* gene-based monotherapy.[19–25] By far, the utility and usefulness of ING4 in gene virotherapy strategy is still poorly understood. In addition to that, as both *ING4* and *TRAIL* genes have their own distinct antitumor mechanisms; this in turn may suppose their possible augmenting benefit in cancer gene combination therapy. However, this later suggestion is also not investigated yet either in HCC or other human cancer modalities.

Hence, we herein generated two OAds encoding human *TRAIL* (Ad-ΔB/TRAIL) and *ING4* (Ad-ΔB/ING4) gene, respectively and then investigated the antitumor activity and safety profile of their mono- and combined therapy on preclinical models of human HCC. Our collective data showed novel evidence that co-therapy with Ad-ΔB/TRAIL and Ad-ΔB/ING4 exhibited more enhanced *in vivo* antitumor activity on an orthotopic model of human HCC than their individual therapy, without inducing overlapping toxicity, and it was closely associated with remarkable induction of antitumor apoptosis and immune response, and suppression of tumor angiogenesis.

RESULTS

OAds efficiently expressed their armed *TRAIL* and *ING4* genes in transfected human HCC cells

A replication competent OAd (Ad-ΔB) armed with human *ING4* gene (Ad-ΔB/ING4), or human *TRAIL* gene (Ad-ΔB/TRAIL), was generated (Figure 1a) and then viral replication and *TRAIL* and *ING4* gene expression were validated *in vitro* on human HuH7 HCC cells treated with phosphate-buffered saline (PBS), Ad-ΔB/TRAIL, Ad-ΔB/ING4 or Ad-ΔB/TRAIL plus Ad-ΔB/ING4 (Ad-ΔB/TRAIL + ING4) at the multiplicity of infection (MOI) of 5 per vector. The treated cells and their supernatants were harvested and analyzed by quantitative reverse transcriptase (qRT)-PCR to measure the mRNA expression of *TRAIL* and *ING4* genes, enzyme-linked immunosorbent assay (ELISA) to quantify TRAIL protein, western blotting assay to detect TRAIL and ING4 protein, and to verify the viral replication by detecting expressed Ad E1A protein in these infected cells. As shown in Figure 1, TRAIL was remarkably expressed at its mRNA (Figure 1b) and protein (Figures 1c and f) levels in HCC cells received Ad-ΔB/TRAIL-based therapy (that is, Ad-ΔB/TRAIL alone or Ad-ΔB/TRAIL + ING4), and the mRNA and protein of ING4 (Figures 1d and e, respectively) were expressed only in cells received *ING4* gene-based therapy (that is, Ad-ΔB/ING4 alone or Ad-ΔB/TRAIL + ING4), indicating that the generated Ad-ΔB vectors had succeeded to deliver their armed *TRAIL* and *ING4* transgenes in the transfected human HCC cells. Likewise, adenoviral E1A protein (Figure 1e) was detected only in cells

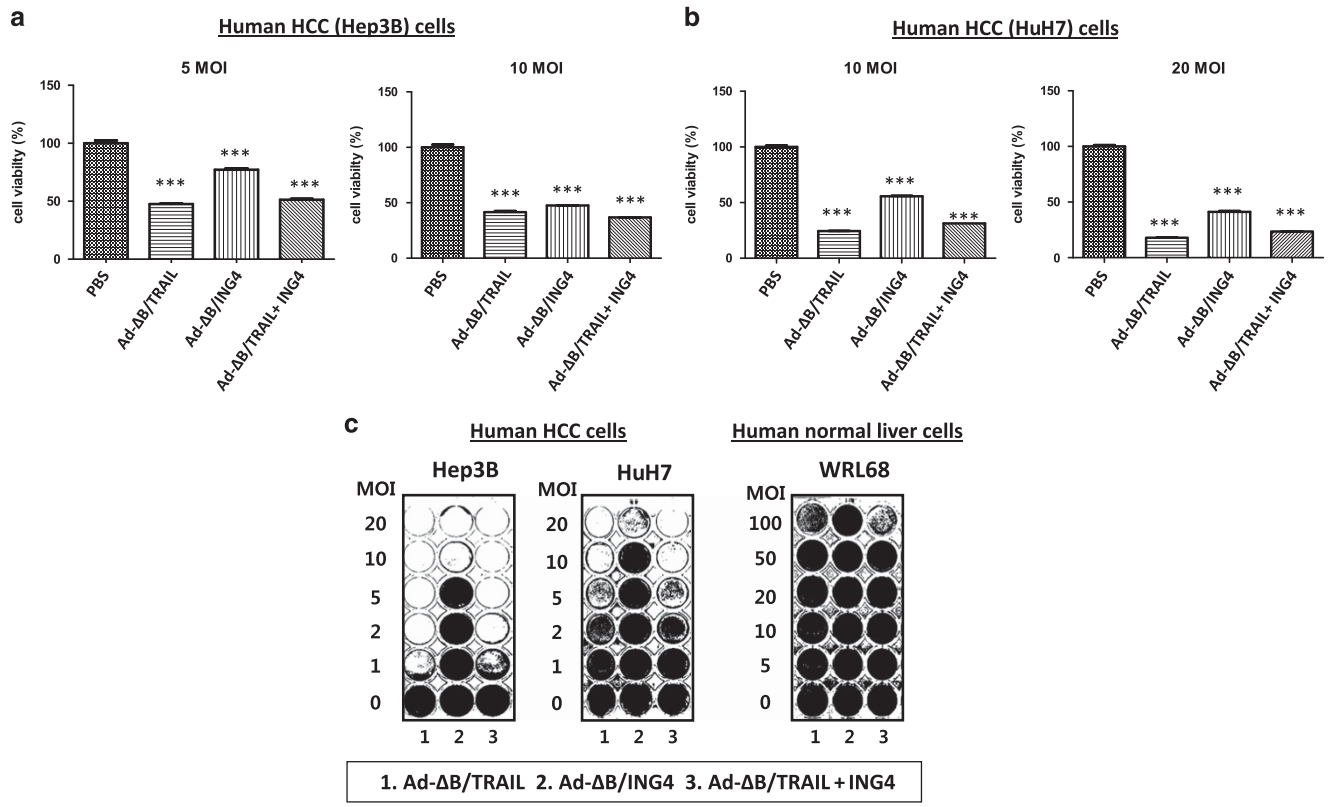

Figure 2. *In vitro* effect of mono- and combined therapy with Ad-ΔB/TRAIL and Ad-ΔB/ING4 on human HCC and normal liver cells. (**a**) Quantitative results of methylthiazolyltetrazolium (MTT) assay showing the inhibitor effects on viability of human HCC (Hep3B) cells treated with 5 and 10 MOI per vector. (**b**) Quantitative results of MTT assay showing the inhibitor effects on viability of human HCC (HuH7) cells treated with 10 and 20 MOI per vector. Data are represented as mean ± s.e. ***$P < 0.001$ versus PBS. (**c**) Representatives of crystal violet staining assay demonstrating the cytotoxic effects on human HCC (Hep3B and HuH7) cells, and on normal human liver (WRL68) cells, at the indicated MOIs of each vector.

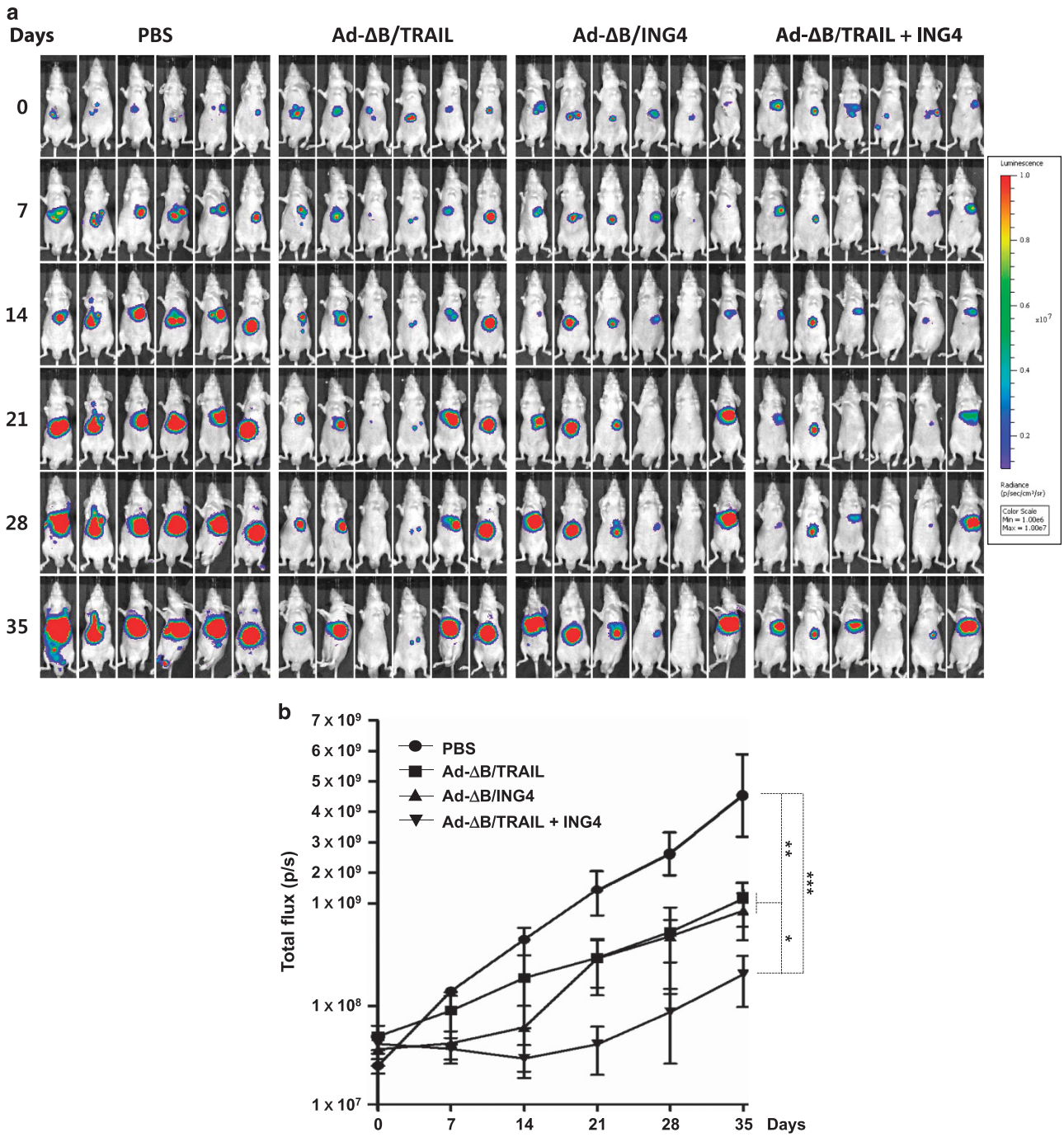

Figure 3. Antitumor effect of mono- and combined therapy with Ad-ΔB/TRAIL and Ad-ΔB/ING4 on orthotopic mouse of human HCC model. The model was established by intrahepatic implantation of 2×10^6 human HCC Hep3B/fluc cells into the liver lobes of athymic nude mice. As described in *Methodology Part*, confirmed positive HCC-bearing mice ($n = 40$) were randomly and equally assigned into four groups and systemically treated with PBS alone (Group 1), Ad-ΔB/TRAIL (Group 2), Ad-ΔB/ING4 (Group 3) and Ad-ΔB/TRAIL + ING4 (Group 4) at a dosage regimen of 1×10^{10} VP in 200 μl PBS of each virus; repeated three times every other day. At day 3 post-treatment, mice of each group were further subdivided into two subgroups: the first subgroup (4 mice/group) was killed and their blood and liver tumor tissues were harvested and used for biochemical, histopathological and mechanistic explorations, while the second one (6 mice/group) was maintained and monitored by *in vivo* bioluminescence imaging (BLI) at days 0, 7, 14, 21, 28, and 35 post-treatment to determine the tumor response rate and the therapeutic effect of each tested treatment strategy. (**a**) Photographed BLI showing tumor growth and its response to each applied treatment. (**b**) BLI signals were calculated after background subtraction in total flux photons/s from a body region of interest. Data presented as mean ± s.e. $^*P < 0.05$, $^{**}P < 0.01$, $^{***}P < 0.001$.

exposed to Ad-ΔB-based therapies (that is, Ad-ΔB/TRAIL, Ad-ΔB/ING4 or Ad-ΔB/TRAIL + ING4) but not in PBS-treated cells (Figure 1e). To further assess *in vitro* replication profile of OAd, human Hep3B HCC cells were seeded in a 12-well plate at 5×10^4 cells per well and infected with Ad-ΔB/TRAIL (0.5 MOI), Ad-ΔB/ING4 (0.5 MOI) or Ad-ΔB/TRAIL (0.25 MOI)+Ad-ΔB/ING4 (0.25 MOI). At 4, 24, and 48 h post-treatment, both supernatant and cells were collected and the copy number of OAd genomes was measured

by Q-PCR (see Supplementary Materials). As shown in Supplementary Figure S4A, the total viral yield increased in a time-dependent manner in these treated Hep3B cells, demonstrating that armed OAd can replicate effectively in human HCC cells.

In vitro antiproliferative and cytopathic effects

Both MTT assay and crystal violet staining assays were performed on two common types of human HCC cell lines, Hep3B and HuH7 cells, to evaluate the *in vitro* anti-HCC killing and cytotoxic effects of the mono- and combined therapy with Ad-ΔB/TRAIL and Ad-ΔB/ING4. Cells were treated with PBS, Ad-ΔB/TRAIL, Ad-ΔB/ING4, or Ad-ΔB/TRAIL + ING4 at indicated MOIs per vector, and their results showed that Ad-ΔB/TRAIL-based therapies (that is, Ad-ΔB/TRAIL alone and Ad-ΔB/TRAIL + ING4), followed by Ad-ΔB/ING4 monotherapy, exhibited dose-dependent and more potent cancer cell killing (Figures 2a, b, and Supplementary Figure S1) and cytopathic (Figure 2c) effects in comparison with Ad-ΔB-treated groups. After that, crystal violet staining assay was also conducted on normal human liver WRL68 cells to validate the *in vitro* safety/toxicity profile of Ad-ΔB/TRAIL and Ad-ΔB/ING4. To cover this goal, the cells were treated with a higher dosage range of Ad-ΔB/ING4, Ad-ΔB/TRAIL or Ad-ΔB/TRAIL + ING4 (0, 5, 10, 20, 50, 100 MOIs per vector). These findings demonstrate a good cancer specificity of the armed OAds as minimal cytotoxicity was observed in normal liver cells (WRL68 cells) at a high dose of 100 MOI, whereas all treatments elicited much higher cytopathic effect at much lower doses (1-20 MOI) in HCC cells (Figure 2c).

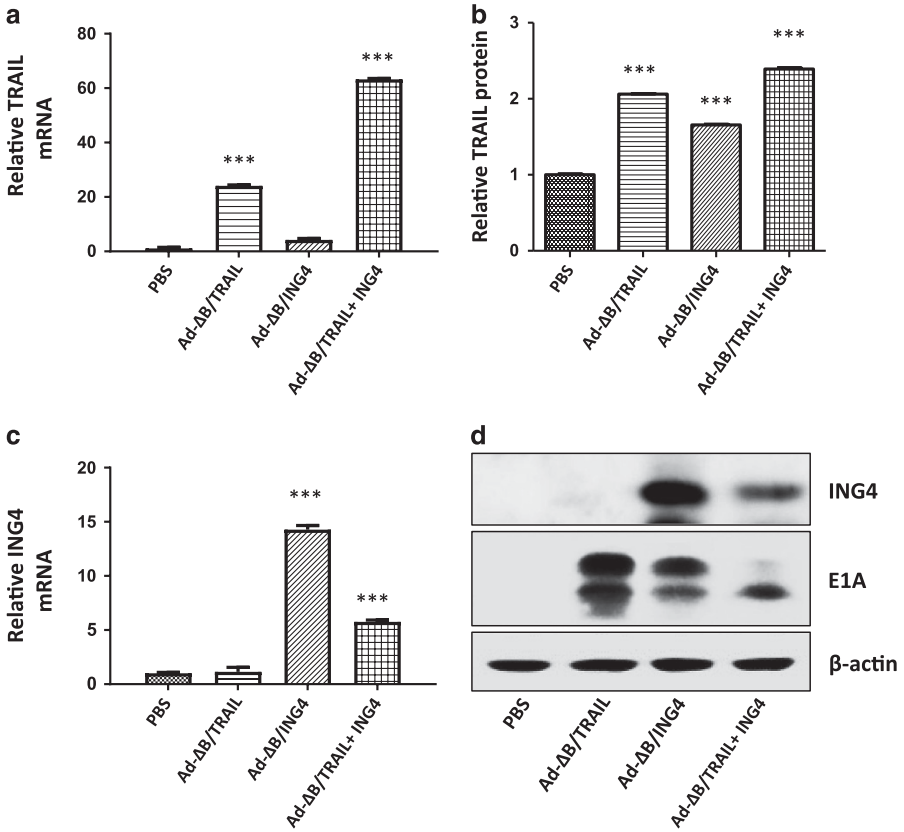

Figure 4. Validation of viral replication and *TRAIL* and *ING4* gene expression in the harvested tumor tissues at day 3 post-treatment. The harvested liver tumor tissues of HCC-bearing mice treated with PBS, Ad-ΔB/TRAIL, Ad-ΔB/ING4 or Ad-ΔB/TRAIL+ ING4 were analyzed by qRT-PCR to measure the relative mRNA levels of *TRAIL* (**a**) and *ING4* (**c**), while the expressed proteins of TRAIL (**b**) and ING4 (**d**) were measured using ELISA and western blot assay, respectively. The expression of Ad E1A protein (as an indicator of viral production) was also assessed by western blot assay (**d**). Data points of (a–c) are mean expression ± s.e. ***$P < 0.001$ versus PBS.

Figure 5. Histopathological, immunological, antiangiogenic and TUNEL findings in the harvested tumor tissues at day 3 post-treatment. The harvested liver tumor tissues of HCC-bearing mice treated with PBS, Ad-ΔB/TRAIL, Ad-ΔB/ING4 or Ad-ΔB/TRAIL + ING4 were subjected to histopathological (H & E staining), immunohistochemical (IHC) staining and *in situ* apoptosis detection by TUNEL assay; and for ELISA assay for intratumoral levels of IFN-γ and VEGF. (**a**) Representative photographs of H & E staining (panel i); IHC staining of CD31-positive vascular endothelial cells (panel ii); and TUNEL staining of apoptotic cells (panel iii) in the harvested tumor tissues of different groups. Original magnification: ×400. (**b**–**d**) are relative intratumoral levels of IFN-γ, VEGF and microvascular density, respectively. Results are mean ± s.e. *$P < 0.05$, ***$P < 0.001$ versus PBS. (**e**) Tumor tissues were stained with anti-DX5 (green) and anti-IFN-γ (red) antibodies to assess intratumoral infiltration of NK cells and their activation. Original magnification, ×200. (**f**) The mean intensity of DX5-positive cells was quantified from three independent fields within five different microscope images for each experimental group. Data are representative of three independent experiments. *$P < 0.05$, **$P < 0.01$ or ***$P < 0.001$ versus PBS-treated group. (**g**) The mean intensity of IFN-γ-positive cells was quantified from three independent fields within five different microscope images for each experimental group. Data are representative of three independent experiments. **$P < 0.01$ or ***$P < 0.001$ versus PBS-treated group. (**h**) The percentage of $DX5^+IFN\text{-}\gamma^+$ NK cells was assessed by ImageJ software. The mean intensity of $DX5^+IFN\text{-}\gamma^+$ NK cells was quantified from three independent fields within five different microscope images for each experimental group. Data are representative of three independent experiments. **$P < 0.01$ or ***$P < 0.001$ versus PBS-treated group.

In vivo antitumor activity on orthotopic mouse model of human HCC

Following *in vitro* studies, an orthotopic model of human HCC was established in the livers of athymic nude mice to evaluate and compare the *in vivo* antitumor therapeutic efficacy and safety of the mono- and combined therapy with Ad-ΔB/TRAIL and Ad-ΔB/ING4. The positively confirmed HCC-bearing mice ($n = 40$) were randomly and equally assigned into PBS (as a control), Ad-ΔB/TRAIL, Ad-ΔB/ING4 and Ad-ΔB/TRAIL + ING4-treated group, at a dosage schedule of 1×10^{10} VP of each vector/injection; three

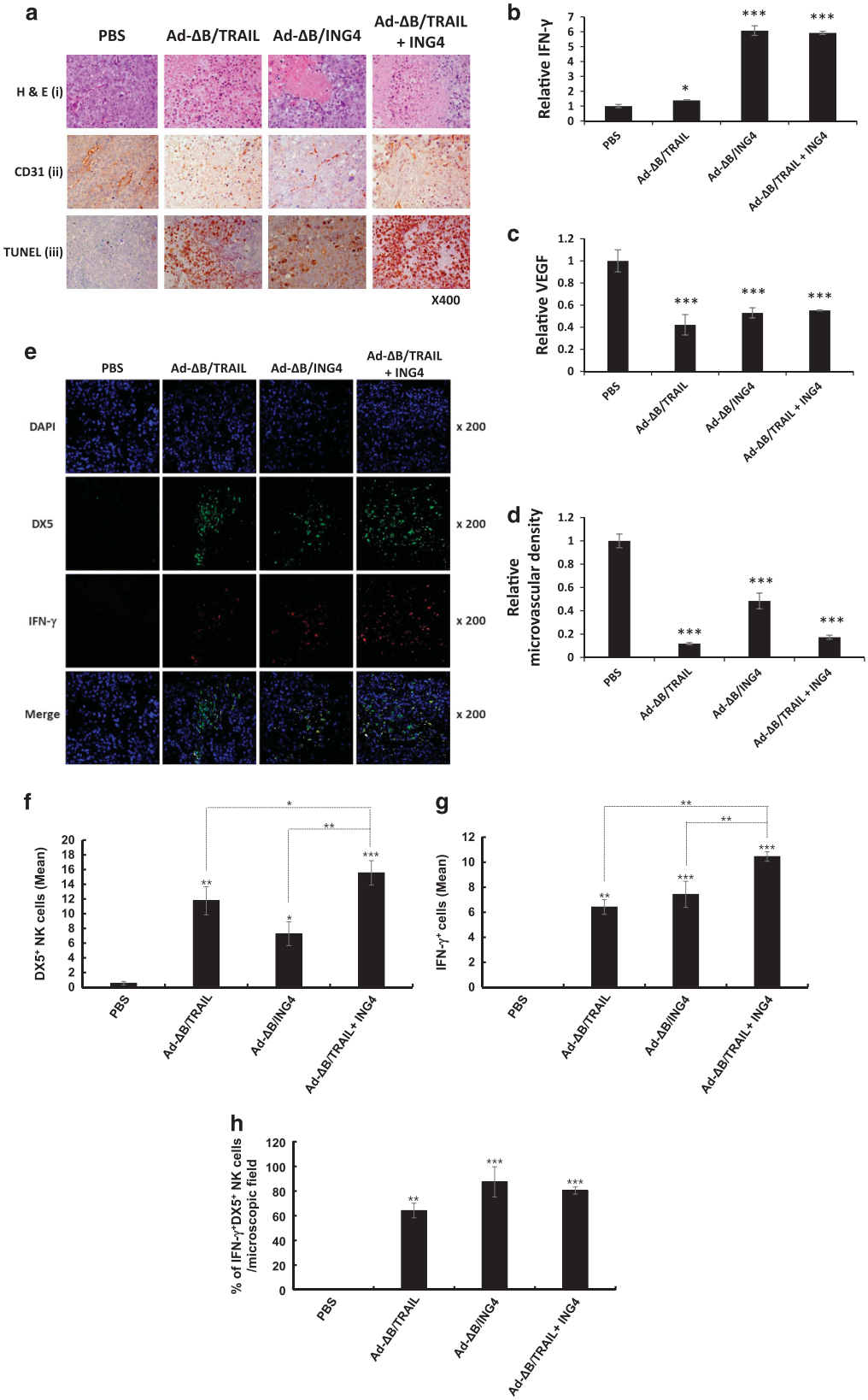

times with 2 days interval. Three days post-treatment, four mice from each group were used for histopathological, biochemical and mechanistic investigations, while the remaining six mice/group were maintained until the end of the study (at day 35 post-treatment) to determine the tumor response toward each therapeutic strategy by their monitoring using *in vivo* tumor bioluminescence imaging (BLI) at days 0, 7, 14, 21, 28 and 35 post-treatment. Systemic treatment with Ad-ΔB/TRAIL + ING4 resulted in higher antitumor activity than either monotherapy using Ad-ΔB/TRAIL or Ad-ΔB/ING4 from day 14 to 35 post treatments (Figure 3 and Supplementary Figure S2; $P < 0.001$ versus PBS, $P < 0.05$ versus Ad-ΔB/ING4 and Ad-ΔB/TRAIL). Next, to verify that these *in vivo* anti-HCC therapeutic effects were due to the administered OAds, the liver tumor tissues that were harvested at day 3 post-treatment from the different treated groups were analyzed by qRT-PCR, ELISA and western blotting assays. As shown in Figure 4, the encoded *TRAIL* and *ING4* genes were highly expressed at their mRNAs (Figures 4a and c, respectively) and proteins (Figures 4b and d, respectively) in the tumor tissues of HCC-bearing mice treated with their corresponding vectors, compared with those treated with PBS. In a constant manner, adenoviral E1A protein, as an indicator of viral replication, was only and clearly detected in tumor tissues of mice received mono- or combined therapy with Ad-ΔB/TRAIL + ING4 (Figure 4d and Supplementary Figure S4B). Furthermore, histopathological examination (H & E) of the harvested tumor tissues (Figure 5a, i) was also in consistent with BLI data and showed the presence of extensive necrosis in the tumor tissues of HCC-bearing mice treated with Ad-ΔB/TRAIL + ING4, in contrast to the large area of the proliferating tumor cells that were observed in the tumor tissues of PBS-treated group. Importantly, the tumor-to-liver ratio, which is an important indicator for the therapeutic efficacy and safety of OAd, in Ad-ΔB/TRAIL + ING4-treated mice was 26.2 ± 2.4, showing preferential replication of OAds in tumor tissues by systemic administration (Supplementary Figure S3). Importantly, all treatments did not induce significant hepatic damage as alanine transaminase/aspartate transaminase levels in all OAd containing groups were similar to those of PBS control group (Table 1), indicating the *in vivo* safety profile of the tested therapeutic strategies. In aggregate, these findings suggest the therapeutic potential of utilizing cancer-targeting dual gene virotherapy strategy mediated by OAds armed with *ING4* and *TRAIL* genes as an effective and safe therapeutic tool for treatment of human HCC; however, further studies are still required for additional verification and realization of its possible clinical translation.

In vivo immunological and antiangiogenic findings in tumor microenvironment

To explore the possible underlying mechanisms behind the achieved *in vivo* anti-HCC therapeutic effects, liver tumor tissues harvested at day 3 post treatments were subjected to immunohistochemical and ELISA analysis to determine the intratumoral recruitment of natural killer (DX5-positive) cells and interferon (IFN)-γ production as important indicators of antitumor immune response. To investigate whether each treatment can promote infiltration and activation natural killer (NK) cells in tumor tissues, we performed immunofluorescence double staining using anti-DX5 and anti-IFN-γ antibodies. As shown in Figures 5e and f, tumors treated with Ad-ΔB/TRAIL ($P < 0.01$), Ad-ΔB/ING4 ($P < 0.05$) or Ad-ΔB/TRAIL + ING4 ($P < 0.001$) showed greater infiltration of NK cells than those treated with PBS. Furthermore, higher quantity of NK cells was detected more extensively throughout the tumor tissues following treatment with Ad-ΔB/TRAIL + ING4 than tumors treated with either Ad-ΔB/TRAIL or Ad-ΔB/ING4 alone ($P < 0.05$ versus Ad-ΔB/TRAIL, $P < 0.01$ versus Ad-ΔB/ING4, respectively). Interestingly, tumor tissues treated with Ad-ΔB/ING4 or Ad-ΔB/TRAIL + ING4 showed higher IFN-γ production and higher co-localization of $DX5^{+}IFN\text{-}\gamma^{+}$ NK cells than those treated with PBS or Ad-ΔB/TRAIL alone (Figures 5b, g, and h), suggesting that ING4 expression may enhance IFN-γ secretion from tumor infiltrating NK. Next, to identify the possible antiangiogenic effects, these tumor tissues were also examined by IHC and ELISA to measure the intratumoral levels of CD31-positive endothelial cells (CD31; Figure 5a, ii), vascular endothelial growth factor (VEGF; Figure 5c), and microvascular density (MVD; Figure 5d), as the key mediators for tumor angiogenesis and neovascularization. Compared with PBS-treated tumors, therapy with Ad-ΔB/TRAIL and Ad-ΔB/ING4 had favorably cooperated to repress the intratumoral expression of these three investigated angiogenic factors (Figures 5a, ii, c, and d). Taken together, it can be speculated that *in vivo* therapy with Ad-ΔB/TRAIL + ING4 had positively interacted to eradicate HCC tumor tissues, in part, by inducing antitumor immune response and inhibiting tumor angiogenesis.

In vitro and *in vivo* apoptotic effects

To estimate further mechanisms, the apoptotic changes that could be induced by Ad-ΔB/TRAIL and/or Ad-ΔB/ING4 on HCC cells and/or tumor tissues were measured. The *in vitro* apoptotic effects on human HCC cells treated with PBS, Ad-ΔB/TRAIL, Ad-ΔB/ING4 or Ad-ΔB/TRAIL + ING4 at MOI of 5 of each armed OAd were investigated by flow cytometry. As shown in Figure 6a, monotherapy with Ad-ΔB/TRAIL or Ad-ΔB/ING4 had resulted in induction of both early (Annexin V and propidium iodide-negative cells) and late (Annexin V and propidium iodide double-positive cells) apoptotic cell population on human HCC cells; however, their combination elicited the most potent effect, approximately 77% of total apoptotic cell population. A similar observation was also reported *in vivo* on the harvested tumor tissues using *in situ* apoptosis terminal deoxynucleotidyl transferase (TdT)-mediated dUTP nick-end labeling (TUNEL) assay (Figure 5a, iii). At the protein level, western blotting assay was

Table 1. *In vivo* biochemical findings

Treatment	*Serobiomarkers of liver function*			*Serobiomarkers of kidney function*	
	ALT (SGPT) (U l^{-1})	*AST (SGOT) (U l^{-1})*	*Bilirubin (mg dl^{-1})*	*BUN (mg dl^{-1})*	*Creatinine (mg dl^{-1})*
PBS	53.5 ± 20.5	148.5 ± 75.6	0.1	27.5 ± 2.1	0.2 ± 0.02
Ad-ΔB/TRAIL	77.5 ± 10.6	293.0 ± 38.4	0.1	33.3 ± 4.0	0.2 ± 0.02
Ad-ΔB/ING4	41.0 ± 4.6	191.3 ± 78.8	0.1	26.0 ± 1.0	0.20 ± 0.01
Ad-ΔB/TRAIL + ING4	54.3 ± 16.9	230.0 ± 109	0.1	29.3 ± 3.5	0.3 ± 0.08

Abbreviations: ALT, alanine transaminase; AST, aspartate transaminase; BUN, blood urea nitrogen. HCC-bearing mice were systemically treated with PBS, Ad-ΔB/TRAIL, Ad-ΔB/ING4 or Ad-ΔB/TRAIL + ING4; at a dosage regimen of 1×10^{10} VP/injection; three times every other day. Serum was obtained at 3 days after last dose of each treatment and was biochemically assessed to measure the circulating levels of hepato-renal function biomarkers.

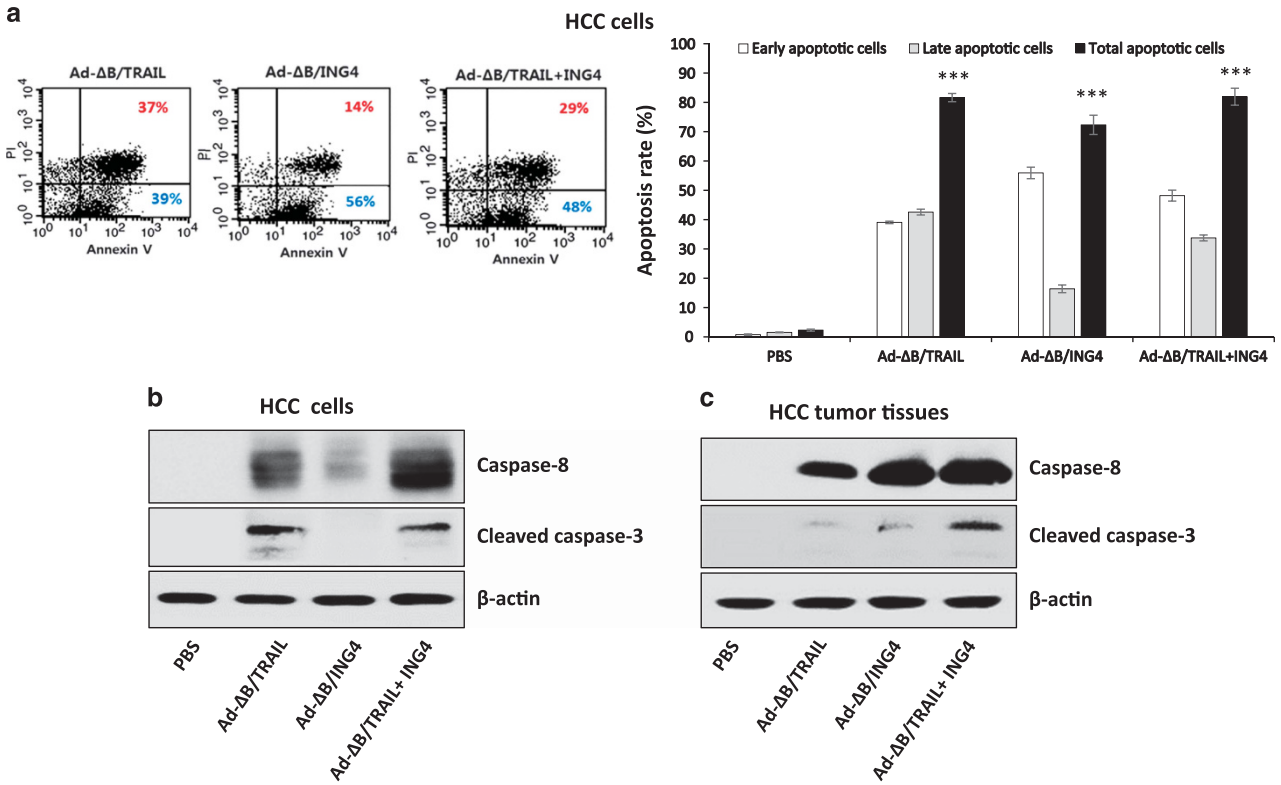

Figure 6. *In vitro* apoptotic findings and expression pattern of caspases-8 and-3 in HCC cells and tumor tissues. (**a**) *In vitro* flow cytometric analysis of apoptosis induction in HCC cells treated with Ad-ΔB/TRAIL, Ad-ΔB/ING4 or Ad-ΔB/TRAIL + ING4 by using Annexin V and propidium iodide (PI) fluorescence staining assay. Each scatter plot demonstrates the percentage of early and late apoptotic cells. ***$P < 0.001$ versus PBS. Next, western blotting analysis of human HCC cells (**b**) and harvested tumor tissues (**c**) treated with PBS, Ad-ΔB/TRAIL, Ad-ΔB/ING4 or Ad-ΔB/TRAIL + ING4 showing the expression pattern of caspase-8 and cleaved caspase-3.

used to measure the expression of caspase-8 and cleaved caspase-3, as well-known apoptosis-inducing molecules, to confirm the induced apoptotic signals. As demonstrated in Figures 6b and c, the combined therapy with Ad-ΔB/TRAIL and Ad-ΔB/ING4 was associated with predominant expression of these two caspases in both HCC cells (Figure 6b) and tumor tissues (Figure 6c), which collectively indicate that facilitation and promotion of antitumor apoptosis was a part in the enhanced tumoricidal effect achieved by Ad-ΔB/TRAIL and Ad-ΔB/ING4 on these preclinical models of human HCC.

DISCUSSION

Development of more effective alternative therapy is an urgent demand for treatment of human HCC.[1,2] Due to their preferential selectivity to replicate in- and kill tumor cells and also their potential success at the preclinical and clinical levels, cancer-targeting gene virotherapy mediated by OAds armed with potential anticancer genes is being the next major breakthrough in this setting.[3–7] ING4 has been lately identified as a potential candidate in gene-based cancer therapy to halt tumor growth and angiogenesis and to facilitate antitumor apoptosis, particularly when combined with additional anticancer gene or drugs.[15,19–25] In despite of this, its beneficial role in OAd-based cancer gene virotherapy is not well investigated yet and remains to be determined. Likewise, to the best of our knowledge there is no previous attention has been given to the potentiality of combining TRAIL; a potent antitumor apoptotic ligand that its importance in cancer combination therapies has been strongly recommended,[8,10,14] with ING4 to improve their overall anticancer response and overcome cancer resistance. To address these interesting issues we therefore generated two OAds: one armed with human *ING4* gene (Ad-ΔB/ING4) and another (with the same viral backbone) armed with *TRAIL* gene (Ad-ΔB/TRAIL), and then investigated their individual and combined antitumor activity, safety profile and underlying mechanisms on preclinical models of human HCC.

The *in vitro* studies of the present research work were conducted on human HCC Hep3B and HuH7 cell lines and also on normal liver (WRL68) cells, while the *in vivo* studies were performed on an orthotopic transplanted model established by intrahepatic implantation of human HCC Hep3B cells in the livers of nude mice. At that respect, human Hep3B and HuH7 cells are well-differentiated human hepatocyte-derived cellular carcinoma cell lines that widely used in investigational and translation therapeutic studies related to human liver cancer.[26,27] Furthermore, while no experimental animal model is expected to completely cover the aggressive behavior and complexity of human HCC, it has been revealed that establishment of an *in vivo* orthotopic cancer model in its target organ is being the most reliable one and its preclinical outcomes are more credible and applicable to clinical translation if compared with subcutaneous xenograft model.[28] Additionally, Ad-ΔB/TRAIL and Ad-ΔB/ING4 were administered systemically and *in vivo* BLI, which is a non-invasive and convenient diagnostic tool with excellent quantitative sensitivity and assessment,[29] was used to monitor tumor growth and estimate the rate of tumor response to each applied therapeutic strategy. Overall, our collective findings demonstrated that combination therapy failed to exert synergistically enhanced cancer cell killing efficacy due to Ad-ΔB/TRAIL eliciting more potent cancer cell killing effect than Ad-ΔB/ING4 *in vitro*, but induced more potent tumor growth inhibition than either monotherapy *in vivo* without observable overlapping toxicity (Table 1). This was likely due to combination therapy modulating multiple components of tumor microenvironment that cannot be emulated *in vitro* two-dimensional culture system. In specific, the combination therapy induced more robust activation

and infiltration of NK cells, induction of apoptosis, and inhibition of angiogenesis and vascularization than monotherapy *in vivo* (Figures 5 and 6). These *in vivo* findings support the previously published considerations that concomitant delivery of *ING4* gene,[19,20,25] and likewise *TRAIL* gene,[8,10,13,14] with another potential tumoricidal gene is more effective in gene-based cancer therapy to overcome cancer resistance, and also re-highlight the importance of OAd in mediating potential cancer-targeting dual gene virotherapy strategy and providing a more meaningful therapeutic maneuver against multigenic and highly resistant cancers, such as HCC, particularly if the two transgenes are well chosen.[7–11] As combination of two viruses is a major challenge for translation relevance compared with use of single virus, a future study should examine a single oncolytic virus co-expressing both *TRAIL* and *ING4* genes to examine whether expression of both genes by a single vector system can still elicit more potent anticancer effect than a control vector expressing single therapeutic gene.

Most hopeful tumoricidal agents eradicate tumor cells by the induction of apoptosis. Therefore, we next measured the apoptotic effects that could be mediated by Ad-ΔB/TRAIL and/or Ad-ΔB/ING4A therapy. The results showed that monotherapy with Ad-ΔB/TRAIL or Ad-ΔB/ING4 had resulted in induction of apoptosis in both HCC cells and tumor tissues and was closely associated with overexpression of caspase-8 and -3, and the most potent effect was achieved with Ad-ΔB/TRAIL and Ad-ΔB/ING4 combination therapy. In agreement, TRAIL is experiencing a renaissance as a highly potent pro-apoptotic ligand that induces fulminant apoptosis in HCC and other human cancer cell types, mainly through activation of the executioner caspase pathway, with negligible effects on normal cells.[12–14] Similarly, a particular advance has been demonstrated with ING4 in inducing apoptotic cell death, particularly via the caspase pathway, in tumor cells but not in normal cells.[19–24,30] Angiogenesis is also a vital process for tumor growth and malignant phenotype, and human HCC is characterized as a hypervascular tumor with a potential target for anti-angiogenesis therapy.[31,32] Mechanistically, activation of VEGF pathway and overexpression of endothelial vascular markers, in particular CD31, have been described as the central angiogenic factors,[7,33] and currently blockade of VEGF pathway is an active investigational approach to suppress HCC and other tumor angiogenesis.[7,31–34] Overexpression of VEGF and CD31-positive cells has been noted in human HCC tissues than their surrounding normal liver tissues.[34] In consistency, an influential positive interaction was observed in the present study between Ad-ΔB/TRAIL and Ad-ΔB/ING4 to repress VEGF, CD31-positive cells and tumor MVD in the liver tumor tissues of the established orthotopic model of HCC. In agreement with our findings, the pivotal antiangiogenic role of ING4 via inhibition of VEGF, CD31, CD34 and MVD has been strongly evidenced.[20,21,24,30] The disseminating effect of OAd on tumor angiogenesis and tumor-driven vasculature has also been reported,[35] and disruption of VEGF pathway was found to increase the amplification and distribution of OAds in tumor microenviroments.[36] TRAIL has also been found to efficiently decrease blood vessel formation and VEGF-induced angiogenesis in the tumor tissues.[37] Therefore, we can speculate this triplex of Ad-ΔB/TRAIL + ING4 was worked together to eradicate the tumor tissues in the livers of HCC-bearing mice by the concomitant induction of apoptosis and halting tumor-driven angiogenesis and neovascularization.

Cancer immune therapy based on NK cells and their released cytotoxic cytokines, in particular IFN-γ, have made some clinical breakthroughs over the recent years.[38] Activated NK cells are able to eliminate both mature tumor cells and the small cancer-initiating cells or cancer stem cells that are poorly recognized by other immune cells and involved in tumor maintenance and recurrence.[39] IFN-γ-based therapy has also been tested on a variety of human malignancies.[40] To explore this immunological aspect here, we assessed the status of NK cells and IFN-γ in the harvested liver tumor tissues of all animal groups, using IHC and ELISA analysis, respectively. The results showed that Ad-ΔB/TRAIL and Ad-ΔB/ING4 in combination can greatly enhance the intratumoral infiltration and activation of NK cells in comparison with either treatment administered alone. Of note, both Ad-ΔB/ING4- and Ad-ΔB/TRAIL + ING4-treated tumors showed markedly higher quantity of IFN-γ-expressing NK cells than those treated with Ad-ΔB/TRAIL, suggesting that expression of ING4 may be crucial for activation of tumor infiltrating NK cells as ING4 overexpression has been reported to inhibit NF-κB-mediated immunosuppression in cancer.[41–44] Additionally, positive correlation between induction of apoptosis (TUNEL-positive spots) and intratumoral infiltration of NK cells were observed, suggesting that expression of TRAIL (Ad-ΔB/ TRAIL or Ad-ΔB/ TRAIL + ING4) could facilitate intratumoral infiltration of immune cells likely through enhanced induction of apoptosis. These findings are in line with previous reports suggesting that apoptosis can be highly immunogenic and promote immune cell infiltration.[45,46] Furthermore, recruitment of NK cells into liver tumor tissues was clinically demonstrated to be directly correlated with good prognosis and survival of HCC patients; and inversely, their exhaustion or dysfunction is a predictor for disease severity and progression.[47] Though the specific role of ING4 in tumor immune-biology is still obscure, TRAIL has been evidenced to be expressed by activated NK and is an important contributor in IFN-γ-dependent NK cell-mediated tumor cells cytotoxicity and protection from tumor growth and metastasis.[48] In addition to NK cells, another subset of immune cells can also produce IFN-γ and mediate TRAIL-dependent lysis of tumor cells.[49] Oncolytic viruses (OVs) have also been recognized as a potent NK cell activator, and these NK cells enhance OV to clear tumors in various instances.[50] In short, such immunological findings may suggest that a circadian crosstalk was created by OAd, ING4 and TRAIL to efficiently recruit cytotoxic NK cells and overproduce IFN-γ in the tumor tissues. As combination of TRAIL and ING4 was able to enhance NK cell infiltration and activation in tumor tissues in comparison with either virus used alone being administered at two-fold higher dose, a future study should examine immunological modulation mediated by combination therapy in greater detail as complex and immunosuppressive tumor microenvironment remains a critical challenge toward successful cancer therapy.

In summary, this is the first study showing the feasibility and efficacy of utilizing OAds simultaneously expressing *ING4* and *TRAIL* genes as a new effective and safe therapeutic approach for treatment of human HCC. In the present study, OAd-mediated *in vivo* co-delivery of *TRAIL* and *ING4* genes confers better tumor control than OAd-delivered *ING4* or *TRAIL* gene alone, and was closely associated with positive interaction to diminish tumor-driven angiogenesis and neovascularization, and to induce antitumor apoptosis and immunity. Additional antitumor mechanisms might be occurred, which in turn requires further explorations studies. We believe that continued exploration of this strategy may provide greater control for other types of devastating human malignant diseases.

MATERIALS AND METHODS

Cell lines and cultures

Hep3B (human HCC cell line), WRL68 (human normal liver cell line) and HEK293 (human embryonic kidney cell line expressing the E1A region of human adenovirus type 5) were from American Type Culture Collection (ATCC, Manassas, VA, USA), while HuH7 (human HCC cell line) was from JCRB Genebank, Osaka, Japan. All cell lines were cultured in Dulbecco's modified Eagle's medium (Thermo Fisher Scientific, Inc., Waltham, MA, USA) supplemented with 10% heat-inactivated fetal bovine serum (Gibco BRL, Grand Island, NY, USA), 2 mmol l^{-1} glutamine, 50 U ml^{-1} penicillin and

50 μg ml^{-1} streptomycin. Cells were maintained at 37 °C in a humidified incubator with 5% CO_2.

Construction and generation of OAds armed with human *ING4* and *TRAIL* transgenes

The viral backbone of a conditionally replicating OAd mutated in E1A and deleted in E1B regions (Ad-ΔB) was generated as previously described.[51] Next, to generate Ad-ΔB armed with either human *ING4* gene (Ad-ΔB/ING4) or human *TRAIL* gene (Ad-ΔB/TRAIL) (Figure 1a), the corresponding DNA region of human *ING4* or *TRAIL* gene was first amplified by PCR using the following primer sets: 5′-CCCAAGCTTATGGCTGCGGGGATGTATTTG-3′ (sense primer) and 5′- CCCAAGCTTCTATTTCTTCTTCCGTTCTTGG -3′ (antisense primer) for *ING4*; and 5′-ATCGCCCGGATTAAGAAA-3′ (sense primer) and 5′-CAAGTGCAAGTTGCTCAGGA-3′ (antisense primer) for *TRAIL*. The amplified PCR products were sub-cloned into pSP72 adenoviral shuttle vector containing the E3 region of human adenovirus type 5 (pSP72-E3; Promega Corp., Madison, WI, USA) to generate a pSP72-ING4 and a pSP72-TRAIL shuttle vector, respectively. The two resultant shuttle vectors were individually linearized with restriction enzyme digestion, co-transformed with Ad-ΔB DNA into *E. coli* BJ5183 cells, and cultured for overnight for homologous recombination. To verify each respective homologous recombinant, the purified plasmid DNA from the cultured *Escherichia coli* was digested with *Hin*dIII restriction enzyme and the digestion pattern was confirmed by PCR analysis. The two homologous plasmid DNA recombinants were further digested with *Pac*I restriction enzyme and transfected into HEK293 cells to generate their corresponding viral particles (Ad-ΔB/ING4 and Ad-ΔB/TRAIL, respectively), and then they were further propagated in HEK293 cells, purified by CsCl gradient density purification method, dissolved in a storage buffer (10 mM Tris, 4% sucrose, 2 mM $MgCl_2$) and stored at − 80 °C until use. The number of viral particles (VP) of purified Ad-ΔB/ING4 and Ad-ΔB/TRAIL viral vectors were calculated from measurements of optical density at 260 nm (OD_{260}), where 1 absorbency unit was equivalent to 1.1×10^{12} VP ml^{-1}. Functional infectious titer (plaque-forming units per milliliter) was determined by limiting dilution assay on HEK293 cells. Finally, the MOI for Ad-ΔB/ING4 or Ad-ΔB/TRAIL was calculated from the infectious titers.

Validation of ING4 and TRAIL expression in transfected HCC cells

HuH7 cells were plated in 24-well culture plates at 4×10^4 cells per well and treated with PBS, Ad-ΔB/TRAIL, Ad-ΔB/ING4 or Ad-ΔB/TRAIL plus Ad-ΔB/ING4 at a MOI of 5 for each vector. The total VP in combination (2.5 MOI of Ad-ΔB/TRAIL plus 2.5 MOI of Ad-ΔB/ING4) was same as those used in monotherapy group (5 MOI of Ad-ΔB/TRAIL or Ad-ΔB/ING4 alone). At 48 h post-treatment, the cells and their supernatants were harvested and analyzed by qRT-PCR assay; to determine TRAIL and ING4 expression pattern at their mRNA levels, ELISA assay; to measure TRAIL expression at its protein level, and western blotting assay; to verify ING4 and TRAIL expression at its protein level and also to validate adenoviral E1A (Ad E1A) protein as an indicator of Ad-ΔB replication in the transfected HCC cells.[52]

RNA isolation, cDNA synthesis and qRT-PCR analysis

Total RNA was extracted from each sample using TRIzol reagent (Gibco BRL) according to the manufacturer's instructions. An equal amount of total RNA (1 μg) was used as a template and reverse-transcribed into cDNA using a first-strand cDNA synthesis kit (Promega Corp.) and under the following conditions: 95 °C for 5 min, 37 °C for 2 h and 75 °C for 15 min. Next, qRT-PCR reaction mixtures were assembled using 50 ng of cDNA, 10 pmol of the aforementioned ING4 or TRAIL primers, and the AmpiGene qPCR Green Mix Lo-ROX (Enzo Life Sciences, Lausen, Switzerland). The reactions were amplified and analyzed in triplicate using the ABI 7500 Real-Time PCR system (Applied Biosystems, Foster City, CA, USA), and 18S ribosomal RNA was used as an internal control.

Protein extraction, western blot and ELISA analysis

Samples were lysed in ice-cold RIPA buffer with a proteinase inhibitor cocktail (Santa Cruz Biotechnology, Inc., Santa Cruz, CA, USA), centrifuged at 15,000 g for 10 min at 4 °C. The protein concentration in each supernatant was measured using the Pierce BCA Protein Assay Kit (Thermo Fisher Scientific, Inc.). Next, western blotting assay was carried by separating equal protein aliquots (20 μg per sample) on a 10 sodium dodecyl sulfate-polyacrylamide gel electrophoresis and transferred to a polyvinylidene fluoride membrane (EMD Millipore, Bedford, MA, USA). Nonspecific binding sites were blocked by incubation of the membranes in TBS-T (50 mM Tris-HCl, pH 7.6, 150 mM NaCl, 0.2% Tween 20) containing 3% bovine serum albumin for 2 h at room temperature. Thereafter, the membranes were incubated overnight at 4 °C with rabbit polyclonal primary antibodies (Santa Cruz Biotechnology, Inc.) against ING4, Ad E1A, TRAIL and β-actin. After washing process with TBS-T, horseradish peroxidase-conjugated anti-rabbit IgG was added and incubated for 45 min at room temperature, followed by 3–5 washes with TBS-T. Visualization of the developed blots was accomplished using enhanced chemiluminescence detection reagents, and normalization was made against β-actin expression. ELISA was performed to quantitatively measure the expression levels of TRAIL protein using conventional TRAIL ELISA kit (BD, San Jose, CA, USA), according to the manufacturer's instructions.

In vitro cell viability (MTT assay)

MTT assay (Sigma, St Louis, MO, USA) was conducted to assess the *in vitro* killing/antiproliferative effects of the singular and combined treatments with Ad-ΔB/TRAIL and Ad-ΔB/ING4 on human HCC cells (Hep3B and HuH7). For the assay, the Hep3B and HuH7 cells were individually plated onto 24-well plates at about 60–70% confluence, and then treated with PBS, Ad-ΔB/TRAIL, Ad-ΔB/ING4 or Ad-ΔB/TRAIL + ING4 at indicated different dosages of each virus (5 and 10 MOIs for Hep3B; 10 and 20 MOIs for HuH7 cells) and then incubated at 37 °C for 48 h. After incubation, 200 μl MTT (2 mg ml^{-1} in PBS) was added to each well, and then incubated at 37 °C for 4 h. Supernatant and cultured medium of each well was aspirated and replaced with 150 μl dimethyl sulfoxide to solubilize the formazan crystals into a colored solution measured at 540 nm using a microplate reader (Bio-Rad 680, Hercules, CA, USA). The experiments were repeated in triplicate, and cell viability in each well was calculated following this formula: cell survival = (absorbance value of treated cells − blank)/(absorbance value of untreated control cells), and expressed as the percentage of untreated control cells.[33]

In vitro cytotoxicity assay

Crystal violet staining assay (Sigma) was performed to further assess the specific growth inhibitory effects mediated by Ad-ΔB/TRAIL and/or Ad-ΔB/ING4 on the human HCC cells (Hep3B and HuH7). In addition to that, this crystal violet staining assay was also employed on normal human liver (WRL68) cells to predict the safety profile of each tested therapeutic strategy. During the assay, Hep3B, HuH7 and WRL68 cells were individually cultured at about 60–70% confluence and then treated with PBS, Ad-ΔB/TRAIL, Ad-ΔB/ING4 or Ad-ΔB/TRAIL + ING4 at various MOIs of each viral vector: 0, 1, 2, 5, 10, 20 MOIs for Hep3B or HuH7 cells; and 0, 5, 10, 20, 50, 100 MOIs for WRL68 cells. Seventy-two hours post-treatment, the culture media of each well was removed and replaced by adding 500 μl of crystal violet solutions (0.5% crystal violet in 50% methanol) for staining process. After 30 min, the wells were smoothly washed with distilled water, naturally dried, then imaged and documented as photographs. The experiments were repeated three times; and PBS-treated cell groups were concurrently analyzed as negative controls.

Flow cytometry and *in vitro* apoptosis study

Flow cytometry and the Annexin V-FITC Apoptosis Detection kit (BioVision, Inc., Milpitas, CA, USA) were used to evaluate *in vitro* apoptotic effects of Ad-ΔB/TRAIL and/or Ad-ΔB/ING4 on human HCC, according to the manufacturer's instructions. In brief, HCC cells were treated with PBS, Ad-ΔB/TRAIL, Ad-ΔB/ING4 or Ad-ΔB/TRAIL + ING4 (at MOI of 5 of each viral vector), and 52 h later, the cells were harvested, washed once with ice-cold complete medium, re-suspended in binding buffer containing 0.5 μg ml^{-1} FITC-labeled Annexin V (as early apoptotic marker) and 0.6 μg ml^{-1} propidium iodide (as late apoptotic marker) and then incubated for 15 min in the dark at room temperature. The stained apoptotic cells were analyzed using a FACScan flow cytometry (BD). The cells were assayed in triplicate and the total apoptotic cell population in each treatment was calculated by the percentage of early apoptotic and late apoptotic cells. Furthermore, as mentioned below western blot assay was also performed to detect the expression of two common apoptosis-related molecules: caspase-3 and -8, in these treated cells.

Animal experiments

In the present study, an orthotopic implantation model of human HCC was established in the livers of 4–5-week-old male BALB/c athymic nude mice. All mice were maintained in laminar flow cabinets under pathogen-free

conditions. Animal care and all *in vivo* experimental procedures were carried out according to the protocols approved by the US Public Health Service Policy on Humane Care and Use of Laboratory Animals. To establish the model, 2×10^6 human Hep3B/fluc cells (ATCC) were suspended in 50 µl of sterile PBS and directly implanted into the parenchyma of their left liver lobe of each mouse using 28-gauge needles as described previously.[26] Fifteen days later, *in vivo* BLI were performed and analyzed to confirm the successfulness of model establishment, in which the mice were anesthetized in a chamber filled with 2% isofluorane in oxygen, injected intraperitoneally with 150 mg kg^{-1} of D-luciferin potassium salt (Caliper Life Sciences, Hopkinton, MA, USA) and after 10 min, BLI were acquired and analyzed using IVIS spectrum imaging system (Xenogen, Alameda, CA, USA). For each mouse, a region of interest was drawn around the tumor and the obtained BLI signals were calculated as the sum of both prone and supine acquisitions after background subtraction total flux (photons per second; p s^{-1}) from a total body region of interest. Mice whose BLI signals reached around 2×10^8 p/s were assigned as positive tumor-bearing animals[26] and then randomly divided into the following four groups ($n=10$/group) and systemically treated with: PBS (Group 1), Ad-ΔB/TRAIL alone (Group 2), Ad-ΔB/ING4 alone (Group 3) and Ad-ΔB/TRAIL + ING4 (Group 4). Ad-ΔB/ING4 and/or Ad-ΔB/TRAIL was injected intravenously through the caudal vein in a dosage schedule of 1×10^{10} VP (1×10^{10} VP/injection for Ad-ΔB/TRAIL or Ad-ΔB/ING4 as monotherapy and 5×10^9 VP of each virus for the combination therapy) repeated total of three times every other day. After treatment, the animals of each group were randomly subdivided into two categories. Mice of the first category (6 mice/group) were maintained and monitored by *in vivo* BLI at days 0, 7, 14, 21, 28 and 35 post-treatment to determine the tumor response rate and the therapeutic effect of each tested treatment strategy, while mice of the second category (4 mice/group) were killed at day 3 post-treatment under sodium pentobarbital general anesthesia (120 mg kg^{-1}, i.p.). Blood samples were collected to be used for measuring the serum levels of hepato-renal function biomarkers (alanine transaminase, aspartate transaminase, bilirubin, blood urea nitrogen and creatinine) as indicators of *in vivo* safety/toxicity profile.[11] Immediately after blood sampling, the liver tumor tissues were harvested and processed for: qRT-PCR, western blotting and ELISA analysis (using the same methodologies as described above) to measure the intratumoral expression levels of *ING4* and *TRAIL* transgenes at their mRNA and protein levels, as well as to validate the intra-tumor adenoviral replication (indexed by Ad E1A protein expression);[52] histopathological, IHC and *in situ* TUNEL apoptosis studies; ELISA assay for measurement the intratumoral levels of IFN-γ and VEGF; and western blotting assay to detect intratumoral expression of caspases -3 and -8.

Histopathological, IHC and TUNEL analysis

Specimens of the tumor tissues of the different groups were fixed in 4% formalin, embedded in paraffin and cut in 4 µm tissue sections. After deparaffinization process, the sections were subjected to (i) the conventional method of hematoxylin and eosin (H&E) staining for histopathological examination; (ii) IHC staining for microvessels (CD31-positive) cells; and (iii) *in situ* apoptosis detection using TUNEL assay. Tissue sections for IHC were dewaxed, rehydrated and processed for antigen retrieval and endogenous peroxidase blocking steps. Following this, the tissue sections were incubated for 30 min in blocking serum and then subjected to staining procedures using monoclonal primary anti-rabbit CD31 (Abcam, Cambrige, MA, USA) antibody, following the manufacturers' protocols, and incubated overnight at 4 °C. Detection of CD31-positive cells was proceeded with incubation of the slides with anti-mouse or anti-rabbit secondary antibody, respectively, followed by streptavidin-peroxidase complex reagent and diaminobenzidine (DAB) chromogen substrate (DAKO, Carpinteria, CA, USA). The tissue sections were then counterstained with Meyer's hematoxylin and dehydrated through a series of ethanol and xylenes. Of note, based on CD31-positive cells, the intratumoral MVD was microscopically counted and calculated in absolute values as previously described.[53] For staining of apoptotic cells in the tissue slides, TUNEL assay was performed using *in situ* apoptosis detection kit (Roche Molecular Biochemicals, Indianapolis, IN, USA) and following the manufacturers' instructions.

Immunofluorescence double staining of tumor tissues with DX5 and IFN-γ antibodies

Tumor sections were prepared as described above for immunofluorescent staining. Tumor sections were stained with a rat anti-mouse DX5 antibody (Biolegend, San Diego, CA, USA) and incubated overnight at 4 °C. Subsequently, the sections were incubated with an Alexa flour 488-labeled chicken anti-rat IgG (Invitrogen, Carlsbad, CA, USA) at room temperature for 2 h. The same sections were then stained with a phycoerythrin-conjugated anti-IFN-γ antibody (BD). For counterstaining, the samples were incubated with 4,6-diamidino-2-phenylindole (DAPI) and observed by a laser scanning confocal microscope (LSM 510-META; Carl Zeiss, Jena, Germany) and then semiquantitatively analyzed by ImageJ software (version 1.50b; US National Institutes of Health, Bethesda, MD, USA).

Assays of caspases-3 and -8, IFN-γ and VEGF

Western blotting assay was performed to detect the expression of caspase-3 and caspase-8 in both human HCC cells and the harvested tumor tissues treated with PBS, Ad-ΔB/TRAIL, Ad-ΔB/ING4 or Ad-ΔB/TRAIL + ING4. During the assay, the cells or tumor tissues were manipulated by the same processes as described above with using rabbit polyclonal IgG primary antibodies against caspases-3 and caspase-8 (Cell Signaling, Danvers, MA, USA), and β-actin as a loading control (Santa Cruz Biotechnology). In addition to that, ELISA-based colorimetric assay kit (R&D Systems, Minneapolis, MN, USA) was used to quantitatively measure the concentrations of IFN-γ and VEGF in the harvested liver tumor tissues of the different treated groups as per the manufacturer's protocol.

Statistical analysis

Data were expressed as mean ± s.e. and statistical analysis was performed using SPSS software version 19.0 (SPSS, Inc., Chicago, IL, USA). Comparison of data between groups was analyzed using one-way analysis of variance (ANOVA), followed by Mann–Whitney test. *P*-values <0.05, <0.01 and <0.001 were considered a statistically significant, very significant and very much significant difference, respectively.

CONFLICT OF INTEREST

The authors declare no conflict of interest.

ACKNOWLEDGEMENTS

This research work was funded by the National Science, Technology and Innovation Plan (MARRIFAH)-King Abdul Aziz City for Science and Technology (KACST), the Kingdom of Saudi Arabia, Award Number (11-MED2065-10, to AGE-S) and the National Research Foundation of Korea (2013M3A9D3045879, 2015R1A2A1A13027811, 2016M3A9B5942352; to C-OY).

AUTHOR CONTRIBUTIONS

Study conception and design: AGE-S and C-OY; experiments, measurements, analysis and interpretation of data: AGE-S, AMA, EO, B-KJ, MB, AA and C-OY; writing and review of the manuscript: AGE-S, AMA, EO, B-KJ, MB, AA and C-OY; and drafting the article to be published: AGE-S and C-OY.

REFERENCES

1 Brito AF, Abrantes AM, Tralhão JG, Botelho MF. Targeting hepatocellular carcinoma: what did we discover so far? *Oncol Rev* 2016; **10**: 302.
2 Gong XL, Qin SK. Progress in systemic therapy of advanced hepatocellular carcinoma. *World J Gastroenterol* 2016; **22**: 6582–6594.
3 Larson C, Oronsky B, Scicinski J, Fanger GR, Stirn M, Oronsky A *et al.* Going viral: a review of replication-selective oncolytic adenoviruses. *Oncotarget* 2015; **6**: 19976–19989.
4 Jebar AH, Errington-Mais F, Vile RG, Selby PJ, Melcher AA, Griffin S. Progress in clinical oncolytic virus-based therapy for hepatocellular carcinoma. *J Gen Virol* 2015; **96**: 1533–1550.
5 Wang YG, Huang PP, Zhang R, Ma BY, Zhou XM, Sun YF. Targeting adeno-associated virus and adenoviral gene therapy for hepatocellular carcinoma. *World J Gastroenterol* 2016; **22**: 326–337.
6 Rosewell Shaw A, Suzuki M. Recent advances in oncolytic adenovirus therapies for cancer. *Curr Opin Virol* 2016; **21**: 9–15.
7 Yuan S, Fang X, Xu Y, Ni A, Liu XY, Chu L. An oncolytic adenovirus that expresses the HAb18 and interleukin 24 genes exhibits enhanced antitumor activity in hepatocellular carcinoma cells. *Oncotarget* 2016; **7**: 60491–60502.

8 Cai Y, Liu X, Huang W, Zhang K, Liu X. Synergistic antitumor effect of TRAIL and IL-24 with complete eradication of hepatoma in the CTGVT-DG strategy. *Acta Biochim Biophys Sin (Shanghai)* 2012; **44**: 535–543.
9 Freytag SO, Barton KN, Zhang Y. Efficacy of oncolytic adenovirus expressing suicide genes and interleukin-12 in preclinical model of prostate cancer. *Gene Therapy* 2013; **20**: 1131–1139.
10 Li S, Qi Z, Li H, Hu J, Wang D, Wang X *et al.* Conditionally replicating oncolytic adenoviral vector expressing arresten and tumor necrosis factor-related apoptosis-inducing ligand experimentally suppresses lung carcinoma progression. *Mol Med Rep* 2015; **12**: 2068–2074.
11 Oh E, Choi IK, Hong J, Yun CO. Oncolytic adenovirus coexpressing interleukin-12 and decorin overcomes Treg-mediated immunosuppression inducing potent antitumor effects in a weakly immunogenic tumor model. *Oncotarget* 2017; **8**: 4730–4746.
12 Hao C, Song JH, His B, Lewis J, Song DK, Petruk KC *et al.* TRAIL inhibits tumor growth but is nontoxic to human hepatocytes in chimeric mice. *Cancer Res* 2004; **64**: 8502–8506.
13 Norian LA, James BR, Griffith TS. Advances in viral vector-based TRAIL gene therapy for cancer. *Cancers (Basel)* 2011; **3**: 603–620.
14 Refaat A, Abd-Rabou A, Reda A. TRAIL combinations: the new 'trail' for cancer therapy (review). *Oncol Lett* 2014; **7**: 1327–1332.
15 Zhou W, Dia S, Zhu H, Song Z, Cai Y, Lee JB *et al.* Telomerase-specific oncolytic adenovirus expressing TRAIL suppresses peritoneal dissemination of gastric cancer. *Gene Therapy* 2017; **24**: 199–207.
16 Cui S, Gao Y, Zhang K, Chen J, Wang R, Chen L. The emerging role of inhibitor of growth 4 as a tumor suppressor in multiple human cancers. *Cell Physiol Biochem* 2015; **36**: 409–422.
17 Guérillon C, Bigot N, Pedeux R. The ING tumor suppressor genes: status in human tumors. *Cancer Lett* 2014; **345**: 1–16.
18 Fang F, Luo LB, Tao YM, Wu F, Yang LY. Decreased expression of inhibitor of growth 4 correlated with poor prognosis of hepatocellular carcinoma. *Cancer Epidemiol Biomarkers Prev* 2009; **18**: 409–416.
19 Yuan S, Jin J, Shi J, Hou Y. Inhibitor of growth-4 is a potential target for cancer therapy. *Tumour Biol* 2016; **37**: 4275–4279.
20 Xie Y, Lv H, Sheng W, Miao J, Xiang J, Yang J. Synergistic tumor suppression by adenovirus-mediated inhibitor of growth 4 and interleukin-24 gene cotransfer in hepatocarcinoma cells. *Cancer Biother Radiopharm* 2011; **26**: 681–695.
21 Xie Y, Sheng W, Miao J, Xiang J, Yang J. Enhanced antitumor activity by combining an adenovirus harboring ING4 with cisplatin for hepatocarcinoma cells. *Cancer Gene Ther* 2011; **18**: 176–188.
22 Xie Y, Zhang H, Sheng W, Xiang J, Ye Z, Yang J. Adenovirus mediated ING4 expression suppresses lung carcinoma cell growth via induction of cell cycle alteration and apoptosis and inhibition of tumor invasion and angiogenesis. *Cancer Lett* 2008; **271**: 105–116.
23 Cao L, Chen S, Zhang C, Chen C, Lu N, Jiang Y *et al.* ING4 enhances paclitaxel's effect on colorectal cancer growth in vitro and in vivo. *Int J Clin Exp Pathol* 2015; **8**: 2919–2927.
24 Xu M, Xie Y, Sheng W, Miao J, Yang J. Adenovirus-mediated ING4 gene transfer in osteosarcoma suppresses tumor growth via induction of apoptosis and inhibition of tumor angiogenesis. *Technol Cancer Res Treat* 2015; **14**: 369–378.
25 Ren X, Liu H, Zhang M, Wang M, Ma S. Co-expression of ING4 and P53 enhances hypopharyngeal cancer chemosensitivity to cisplatin in vivo. *Mol Med Rep* 2016; **14**: 2431–2438.
26 Kwon OJ, Kim PH, Huyn S, Wu L, Kim M, Yun CO. A hypoxia- and {alpha}-fetoprotein-dependent oncolytic adenovirus exhibits specific killing of hepatocellular carcinomas. *Clin Cancer Res* 2010; **16**: 6071–6082.
27 Donelan W, Li S, Wang H, Lu S, Xie C, Tang D *et al.* Pancreatic and duodenal homeobox gene 1 (Pdx1) down-regulates hepatic transcription factor 1 alpha (HNF1α) expression during reprogramming of human hepatic cells into insulin-producing cells. *Am J Transl Res* 2015; **7**: 995–1008.
28 Lee TK, Na KS, Kim J, Jeong HJ. Establishment of animal models with orthotopic hepatocellular carcinoma. *Nucl Med Mol Imaging* 2014; **48**: 173–179.
29 Thompson SM, Callstrom MR, Knudsen BE, Anderson JL, Sutor SL, Butters KA *et al.* (2013). Molecular bioluminescence imaging as a noninvasive tool for monitoring tumor growth and therapeutic response to MRI-guided laser ablation in a rat model of hepatocellular carcinoma. *Invest Radiol* 2013; **48**: 413–421.
30 Ma Y, Cheng X, Wang F, Pan J, Liu J, Chen H *et al.* ING4 inhibits proliferation and induces apoptosis in human melanoma A375 cells via the Fas/Caspase-8 apoptosis pathway. *Dermatology* 2016; **232**: 265–272.
31 Berretta M, Rinaldi L, Di Benedetto F, Lleshi A, De ReV, Facchini G *et al.* Angiogenesis inhibitors for the treatment of hepatocellular carcinoma. *Front Pharmacol* 2016; **7**: 428.
32 Shen Z, Yao C, Wang Z, Yue L, Fang Z, Yao H *et al.* Vastatin, an endogenous antiangiogenesis polypeptide that is lost in hepatocellular carcinoma, effectively inhibits tumor metastasis. *Mol Ther* 2016; **24**: 1358–1368.
33 Choi IK, Shin H, Oh E, Yoo JY, Hwang JK, Shin K *et al.* Potent and long-term antiangiogenic efficacy mediated by FP3-expressing oncolytic adenovirus. *Int J Cancer* 2015; **137**: 2253–2269.
34 Dhar DK, Naora H, Yamanoi A, Ono T, Kohno H, Otani H *et al.* Requisite role of VEGF receptors in angiogenesis of hepatocellular carcinoma: a comparison with angiopoietin/Tie pathway. *Anticancer Res* 2002; **22**: 379–386.
35 Saito Y, Sunamura M, Motoi F, Abe H, Egawa S, Duda DG *et al.* Oncolytic replication-competent adenovirus suppresses tumor angiogenesis through preserved E1A region. *Cancer Gene Ther* 2006; **13**: 242–252.
36 Thaci B, Ulasov IV, Ahmed AU, Ferguson SD, Han Y, Lesniak MS. Anti-angiogenic therapy increases intratumoral adenovirus distribution by inducing collagen degradation. *Gene Therapy* 2013; **20**: 318–327.
37 Na HJ, Hwang JY, Lee KS, Choi YK, Choe J, Kim JY *et al.* TRAIL negatively regulates VEGF-induced angiogenesis via caspase-8-mediated enzymatic and non-enzymatic functions. *Angiogenesis* 2014; **17**: 179–194.
38 Souza-Fonseca-Guimaraes F. NK cell-based immunotherapies: awakening the innate anti-cancer response. *Discov Med* 2016; **21**: 197–203.
39 Tallerico R, Garofalo C, Carbone E. A new biological feature of natural killer cells: the recognition of solid tumor-derived cancer stem cells. *Front Immunol* 2016; **7**: 179.
40 Miller CH, Maher SG, Young HA. Clinical use of interferon-gamma. *Ann NY Acad Sci* 2009; **1182**: 69–79.
41 Karin M. Nuclear factor-kappaB in cancer development and progression. *Nature* 2006; **441**: 431–436.
42 Karin M, Greten FR. NF-kappaB: linking inflammation and immunity to cancer development and progression. *Nat Rev Immunol* 2005; **5**: 749–759.
43 Tato CM, Mason N, Artis D, Shapira S, Caamano JC, Bream JH *et al.* Opposing roles of NF-kappaB family members in the regulation of NK cell proliferation and production of IFN-gamma. *Int Immunol* 2006; **18**: 505–513.
44 Byron SA, Min E, Thal TS, Hostetter G, Watanabe AT, Azorsa DO *et al.* Negative regulation of NF-κB by the ING4 tumor suppressor in breast cancer. *PLoS One* 2012; **7**: e46823.
45 Zitvogel L, Kepp O, Senovilla L, Menger L, Chaput N, Kroemer G. Immunogenic tumor cell death for optimal anticancer therapy: the calreticulin exposure pathway. *Clin Cancer Res* 2010; **16**: 3100–3104.
46 Demaria S, Volm MD, Shapiro RL, Yee HT, Oratz R, Formenti SC *et al.* Development of tumor-infiltrating lymphocytes in breast cancer after neoadjuvant paclitaxel chemotherapy. *Clin Cancer Res* 2001; **7**: 3025–3030.
47 Sun C, Sun HY, Xiao WH, Zhang C, Tian ZG. Natural killer cell dysfunction in hepatocellular carcinoma and NK cell-based immunotherapy. *Acta Pharmacol Sin* 2015; **36**: 1191–1199.
48 Smyth MJ, Cretney E, Takeda K, Wiltrout RH, Sedger LM, Kayagaki N *et al.* Tumor necrosis factor-related apoptosis-inducing ligand (TRAIL) contributes to interferon gamma-dependent natural killer cell protection from tumor metastasis. *J Exp Med* 2001; **193**: 661–670.
49 Taieb J, Chaput N, Ménard C, Apetoh L, Ullrich E, Bonmort M *et al.* A novel dendritic cell subset involved in tumor immunosurveillance. *Nat Med* 2006; **12**: 214–219.
50 Woller N, Gürlevik E, Ureche CI, Schumacher A, Kühnel F. Oncolytic viruses as anticancer vaccines. *Front Oncol* 2014; **4**: 188.
51 Huang JH, Zhang SN, Choi KJ, Choi IK, Kim JH, Lee MG *et al.* Therapeutic and tumor-specific immunity induced by combination of dendritic cells and oncolytic adenovirus expressing IL-12 and 4-1BBL. *Mol Ther* 2010; **18**: 264–274.
52 Jiang G, Zhang K, Jiang AJ, Xu D, Xin Y, Wei ZP *et al.* A conditionally replicating adenovirus carrying interleukin-24 sensitizes melanoma cells to radiotherapy via apoptosis. *Mol Oncol* 2012; **6**: 383–391.
53 Yoo JY, Kim JH, Kim J, Huang JH, Zhang SN, Kang YA *et al.* Short hairpin RNA-expressing oncolytic adenovirus-mediated inhibition of IL-8: effects on anti-angiogenesis and tumor growth inhibition. *Gene Therapy* 2008; **15**: 635–651.

Supplementary Information accompanies this paper on Gene Therapy website (http://www.nature.com/gt)